Maintaining coherent oscillations in a solid-state qubit via continuous quantum feedback control

Rusko Ruskov, Qin Zhang, and Alexander N. Korotkov

University of California, Riverside, CA 92521

ABSTRACT

We discuss the operation of the one-qubit quantum feedback loop, which may be used for initialization of a qubit in a solid-state quantum computer. The continuous monitoring of a quantum state, which makes the feedback possible, is done by means of a weak continuous measurement and processing of the obtained information via quantum Bayesian equations. The properly designed quantum feedback loop can keep the desired phase of a single-qubit quantum coherent oscillations for infinitely long time, even in presence of a dephasing environment. Various nonidealities reduce the fidelity of the feedback synchronization. We report our study of the effects of finite available bandwidth and time delay on the one-qubit quantum feedback performance, and also discuss the effect of environment-induced dephasing.

Keywords: Continuous quantum measurement, Quantum feedback

1. INTRODUCTION

Protection of quantum information against decoherence is the most challenging task in quantum computation and quantum information processing.[1,2] Quantum error correction[3] is considered at present as the main way to solve this problem. Quantum error correction can be considered as a kind of quantum feedback procedure in which the results of some measurements are used to control the further evolution of the quantum system. In contrast to usual in engineering continuous feedback control, this procedure is rather a discrete feedback based on periodic instantaneous "strong" projective measurements.[4] Nevertheless, continuous quantum feedback can also be used for quantum error correction.[5] Another, more natural, application of continuous quantum feedback is for initialization of qubits in a quantum computer in order to protect the qubits from decoherence before the start of computation.

In physical reality no measurement is instantaneous and of infinite precision.[6] It is especially true in the solid-state domain where the measurement is typically weak and continuous in time.[7] Still, given a continuous measurement record $I(t)$ (for example, a noisy detector current) it is possible to update continuously our knowledge about the system using quantum Bayesian equations.[8,9] The gradual acquisition of information implies that the collapse also happens gradually, while the monitored quantum state undergoes stochastic evolution that reflects the stochasticity of the continuous measurement record. The approach of continuous quantum monitoring via continuous measurement was well developed in quantum optics a decade ago[10,11] as the formalism of quantum trajectories. Recently it was also applied to the solid-state problems[12] and shown to be equivalent[12] to the Bayesian formalism.[9]

The Bayesian formalism has been used for the analysis of the quantum feedback control of a solid-state qubit.[13] It has been shown that the fidelity of maintaining quantum coherent (Rabi) oscillations for an infinitely long time may reach 100% if an ideal (with 100% quantum efficiency) solid-state detector is used. It has been also shown that the quantum feedback can operate even in presence of dephasing due to environment, so that this procedure can be naturally used for the qubit initialization in a solid-state quantum computer. Initialization of fully entangled pair of solid-state qubits using continuous measurement has been analyzed in Ref.[14] . The proposed there procedure needs to use the discrete feedback since the probability of obtaining the entangled state in one run is less than 100% and also since the two-qubit state may switch to a non-entangled state due to various imperfections.

In this paper we study the one-qubit quantum feedback and extend the results of Ref.[13] . In particular, we analyze the performance of the quantum feedback loop in presence of a significant decoherence due to environment, study the effect of a finite bandwidth (which is modelled by averaging the detector signal with a rectangular

Quantum Information and Computation II, edited by Eric Donkor, Andrew R. Pirich, Howard E. Brandt, Proceedings of SPIE Vol. 5436 (SPIE, Bellingham, WA, 2004)
0277-786X/04/$15 · doi: 10.1117/12.542780

time window), and analyze the feedback loop operation in presence of time delay. Our results show that extra decoherence and finite signal bandwidth worsen the performance of the feedback loop; however, the loop does not loose the stability of operation. In contrast, there is a stability threshold for the feedback in presence of a time delay, above which the loop operation becomes unstable.

2. MODEL DESCRIPTION

As the main example of the continuously measured qubit we consider a double quantum dot (DQD) measured by a low-transparency quantum point contact (QPC).[15] All parts of this setup have been demonstrated experimentally.[16] (A somewhat similar setup is the single-Cooper-pair box measured by a single electron transistor (SET) – see, e.g. experiments[17] .) We assume that the DQD is occupied by a single electron and represents a qubit. On the contrary, the QPC is a system with many degrees of freedom and one may consider the detector output (noisy detector current $I(t)$) as a (quasi) classical quantity (the values of the noise at different moments of time are not correlated). If the electron is in dot 2, which is closer to the QPC (we denote the corresponding localized state as $|2\rangle$) then the QPC barrier is higher and so the average current I_2 through the QPC is smaller then the average current I_1 corresponding to the electron location in dot 1 (state $|1\rangle$). Therefore, from the detector current one gets information about the electron location. Typical solid-state realization implies weak response of the detector: $\Delta I = I_1 - I_2 \ll I_0 \equiv (I_1 + I_2)/2$. Due to presence of current noise, a finite measurement time $t \geq \tau_{meas} = 2S_0/(\Delta I)^2$ is necessary to distinguish between the two average currents ($S_0 = 2eI_0$ is the detector current spectral density). For a weakly responding detector many electrons $[\tau_{meas}/(e/I_0) \gg 1]$ pass through the detector during τ_{meas}, and the current can be considered as continuous on the measurement time scale.

The qubit is characterized by the Hamiltonian $\mathcal{H}_{QB} = \varepsilon/2\,(a_2^\dagger a_2 - a_1^\dagger a_1) + H\,(a_1^\dagger a_2 + a_2^\dagger a_1)$, where ε is the energy asymmetry parameter, H characterizes the strength of tunneling between the two states, while $a_{1,2}^\dagger$ and $a_{1,2}$ are the corresponding creation and annihilation operators. The standard Hamiltonian evolution leads to quantum coherent (Rabi) oscillations[18] with the Rabi frequency $\Omega = (4H^2 + \varepsilon^2)^{1/2}/\hbar$. However, the qubit interaction with environment gradually destroys the oscillations[7] that leads to the non-oscillating fully mixed stationary state.

To describe the effect of continuous measurement onto the qubit state evolution, we use the quantum Bayesian formalism.[9] Within this formalism the effect of measurement during small time dt is calculated by applying the Bayes formula from the classical probability theory[19] to the diagonal elements of the qubit density matrix ρ_{ij}, while for an ideal measurement the degree of qubit coherence is conserved (in particular, a pure state remains pure). The procedure is a straightforward generalization of the "orthodox" projection postulate[4] to the case of continuous measurement. In the corresponding Bayesian stochastic differential equations for ρ_{ij}, the unitary part due to the Hamiltonian of the system is supplemented with non-unitary evolution that explicitly contains the measurement record $I(t)$:

$$\dot\rho_{11} = -\dot\rho_{22} = -2\,\frac{H}{\hbar}\,\mathrm{Im}\,\rho_{12} + \rho_{11}\rho_{22}\,\frac{2\Delta I}{S_0}\,[I(t) - I_0], \tag{1}$$

$$\dot\rho_{12} = \mathrm{i}\,\frac{\varepsilon}{\hbar}\,\rho_{12} + \mathrm{i}\,\frac{H}{\hbar}\,(\rho_{11} - \rho_{22}) - (\rho_{11} - \rho_{22})\frac{\Delta I}{S_0}\,[I(t) - I_0]\,\rho_{12} - \gamma\rho_{12}\,, \tag{2}$$

where $\gamma = \gamma_d + \gamma_e$ is the dephasing rate due to detector nonideality (γ_d) and coupling with the environment (γ_e). The dephasing rate $\gamma_d = (\eta^{-1} - 1)(\Delta I)^2/4S_0$ depends on the detector efficiency (ideality) η and vanishes in the ideal case $\eta = 1$, which corresponds to a detector with quantum-limited sensitivity. Theoretically, the QPC is an ideal detector[9] and the SET may also reach the quantum ideality limit.[20, 21] Individual realizations of the measurement process can be simulated using the formula

$$I(t) - I_0 = (\rho_{11} - \rho_{22})\Delta I/2 + \xi(t), \tag{3}$$

where $\xi(t)$ is the pure white noise with spectral density $S_\xi = S_0$. If the Eqs.(1)–(2) are averaged over $\xi(t)$ (the above equations are written in the Stratonovich form[22]), then we obtain usual ensemble-averaged equations: terms proportional to ΔI will disappear and γ will be replaced by ensemble averaged dephasing rate $\Gamma = \gamma + (\Delta I)^2/4S_0$ that is larger than γ because of different evolution of the ensemble members due to random $I(t)$.

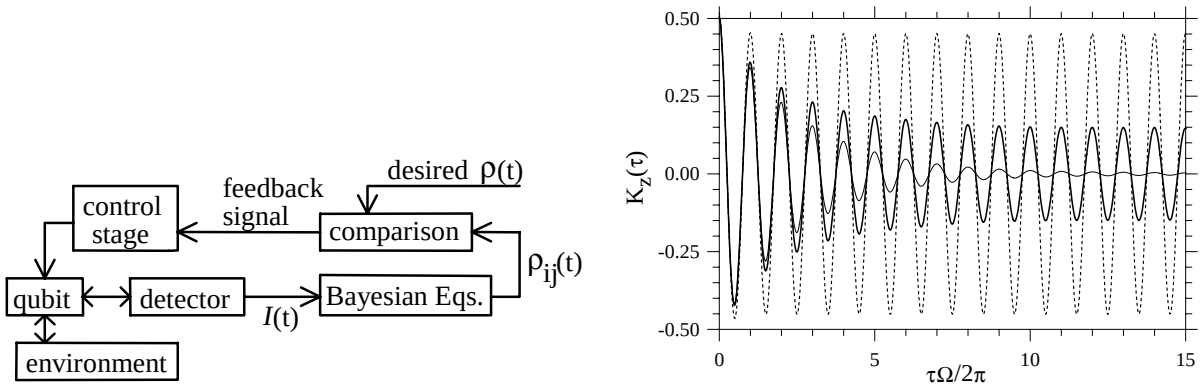

Figure 1. (a) (left panel) Schematic of continuous quantum feedback loop maintaining the desired phase of quantum coherent oscillations of a qubit. (b) (right panel) Correlation function $K_z(\tau)$ of the qubit coherent oscillations for $\mathcal{C} = 1$ and feedback factors $F = 0$ (thin solid line), 0.05 (thick solid line), and 0.5 (dashed line).

3. ONE-QUBIT QUANTUM FEEDBACK CONTROL

A *closed feedback loop* (Fig. 1a) can be organized by monitoring the qubit evolution using the actual measurement result $I(t)$ plugged into Eqs. (1)–(2). The difference between the monitored qubit state and a desired state is used to determine the varying in time correction to the qubit's Hamiltonian, intended to decrease this difference. As in Ref.[13] , we consider the case of a symmetric qubit, $\varepsilon = 0$ (the asymmetry parameter for a charge qubit may be easily set to zero in an experiment), and so the desired evolution is $\rho_{d,11}(t) = 1 - \rho_{d,22}(t) = [1 + \cos(\Omega t)]/2$, $\rho_{d,12}(t) = \rho^*_{d,21}(t) = \mathrm{i}\sin(\Omega t)/2$, where the frequency is $\Omega = 2H/\hbar$. The phase difference $\Delta\phi = \phi - \phi_0$ ($|\Delta\phi| < \pi$) between the monitored value $\phi(t) \equiv \arctan\{2\,\mathrm{Im}\rho_{12}(t)/[\rho_{11}(t) - \rho_{22}(t)]\}$ and the desired phase $\phi_0(t) = \Omega t \pmod{2\pi}$ is treated as the difference ("error") signal, and is used to control the qubit parameter H (changing the barrier height of the DQD). A *linear control* is studied[13]:

$$H_{fb} = (1 - F \times \Delta\phi)H, \tag{4}$$

where F is the dimensionless feedback factor. Qualitatively, the feedback is designed to compensate the phase difference that arises in the process of measurement. If $\Delta\phi > 0$, then $H_{fb} < H$ and the frequency of oscillations decreases, thus reducing the phase difference. The case of negative $\Delta\phi$ is similar.

Let us start with the case of ideal detector, $\eta = 1$, no environment dephasing, $\gamma_e = 0$, infinite bandwidth of the line carrying detector current, $\tau_a = 1/\Delta\omega = 0$, and absence of any time delay, $\tau_d = 0$. Figure 1b shows an example of the feedback performance for moderately weak coupling between qubit and detector: $\mathcal{C} \equiv \hbar(\Delta I)^2/S_0 H = 1$ (the Q-factor of oscillations[23] is equal to $8/\mathcal{C}$, so $\mathcal{C} = 1$ is still a weak coupling). The correlation function $K_z(\tau) = \langle z(t+\tau)z(t)\rangle$ shown in Fig. 1b [$z(t) \equiv \rho_{11} - \rho_{22}$] is calculated numerically using the Monte Carlo simulations[9] of the measurement process for several feedback factors: $F = 0$, 0.05, and 0.5. The correlation function decays to zero without feedback, while for finite feedback factor the correlations remain for infinitely long time. It means the quantum feedback loop really provides the synchronization of quantum oscillations with a classical oscillating signal [full synchronization would correspond to $K_z(\tau) = \cos(\Omega\tau)/2$].

Analytical analysis has been performed in the ideal case $\gamma_d = \gamma_e = 0$, when the qubit state eventually becomes pure[9] (even though the phase of qubit oscillations slowly "diffuses" in time). Simplifying the Bayesian equations (1)–(2) and using the linear control, Eq.(4), we derive stochastic non-linear equation for the phase difference:

$$\frac{d}{dt}\Delta\phi = -\sin\phi\,\frac{\Delta I}{S_0}\left(\frac{\Delta I}{2}\cos\phi + \xi(t)\right) - \frac{2FH}{\hbar}\Delta\phi, \tag{5}$$

which assumes the absence of 2π phase slips. Since we are mainly interested in the weak coupling regime ($\mathcal{C}/8 \ll 1$), the first term in parentheses can be neglected. An averaging of the random term over $\sin\phi$ (for weak

coupling we assume almost harmonic evolution) leads to the simplified equation

$$\frac{d}{dt}\Delta\phi = \tilde{\xi}(t) - \frac{2FH}{\hbar}\Delta\phi, \tag{6}$$

where $\tilde{\xi}(t)$ is an effective white noise with spectral density $S_{\tilde{\xi}} = (\Delta I)^2/2S_0$. This equation describes a particle diffusion in the parabolic potential. The corresponding Fokker-Planck equation has an exact solution which is used to calculate the correlation function $K_z(\tau) \approx \langle\cos[\Delta\phi(t) - \Delta\phi(t+\tau)]\rangle \cos\Omega\tau/2$. In this way we obtain the analytical expression

$$K_z(\tau) = \frac{\cos\Omega\tau}{2}\,\exp\left[\frac{\mathcal{C}}{16F}\left(e^{-2FH\tau/\hbar} - 1\right)\right], \tag{7}$$

which fits well the Monte-Carlo results when $\mathcal{C}/8 \ll 1$ and $\mathcal{C}/16F \leq 1$ (weak coupling and moderate or good synchronization).

Besides the correlation function, we have studied one more characteristic, D, of the synchronization degree. We define D as the time-average scalar product of the unity-length vector on the Bloch sphere corresponding to the desired state, and the vector corresponding to the actual state of the qubit. The equivalent definition is $D \equiv 2\langle \mathrm{Tr}\rho\rho_d\rangle - 1$, where ρ_d is the density matrix of the desired pure state. The usual definition of fidelity is equal to $(D+1)/2$. We use D instead of fidelity because for complete absence of synchronization $D = 0$, while the fidelity is still 0.5. Perfect synchronization corresponds to $D = 1$. Upper solid lines in Fig. 2a and Fig. 3 show the dependence of D on the feedback factor F for $\mathcal{C} = 1$, $\tau_a = 0$, and $\gamma = 0$. One can see that D is proportional to F for small F ("soft" onset of the synchronization) and D is asymptotically approaching 1 at large F. The analytical result

$$D = \exp(-\mathcal{C}/32F) \tag{8}$$

(dashed line in Fig. 3) which follows from Eq. (7), is very close to the numerical results at moderate and good synchronization.

Notice that our result on the possibility of full synchronization is not quite obvious, since the process of measurement changes the qubit state in a random manner, and in some sense the amount of disturbance is equal to the amount of acquired information. Nevertheless, as we will see in the next subsection, the efficient synchronization of qubit coherent oscillations is possible *even in the presence of dephasing environment* if the coupling with the environment is much smaller than the coupling with the detector, and the detector is nearly ideal.

3.1. Quantum Feedback Control in the Presence of Environmental Dephasing

An important feature of the quantum feedback is the ability to suppress the effect of the qubit dephasing caused by interaction with the environment (see Fig. 1a). This can be used, for example, for qubit initialization in a solid-state quantum computer. Solid lines in Fig. 2a show the dependence $D(F)$ for several magnitudes of the dephasing due to environment, $d_e = 0$, 0.1, and 0.5, where $d_e \equiv \gamma_e/[(\Delta I)^2/4S_0]$ is the ratio between the qubit coupling to the environment and to the detector. (We still assume an ideal detector; however, it is very simple to include finite detector efficiency η just using the total dephasing $d_{tot} = d_e + \eta^{-1} - 1$ instead of d_e.) First of all, we see that the feedback still maintains the qubit phase synchronization for infinitely long time. However, for finite d_e the degree of synchronization D saturates at a level less than unity. The dots in Fig. 2b show the saturation value D_{max} as a function of d_e for $\mathcal{C} = 1$, $\tau_a = 0$, and $\eta = 1$. A linear dependence is found at small d_e: $D_{max} \simeq 1 - 0.5\,d_e$. A little better formula

$$D_{max} \simeq 1 - 0.5\,d_e/(1+d_e) \tag{9}$$

[shown by dashed line in Fig. 2b] works reasonably well up to $d_e \leq 1$. (We have also studied the cases $\mathcal{C} = 1/2$ and $\mathcal{C} = 2$, and found that the same formula still works well). These results show that the feedback loop can efficiently suppress the qubit dephasing due to the coupling to the environment if this coupling is much weaker than the qubit coupling to a nearly ideal detector. Surprisingly, our numerical simulations show that even if the dephasing is an order of magnitude stronger than coupling to a nearly ideal detector, the feedback still provides significant ($\sim 40\%$) synchronization of quantum coherent oscillations.

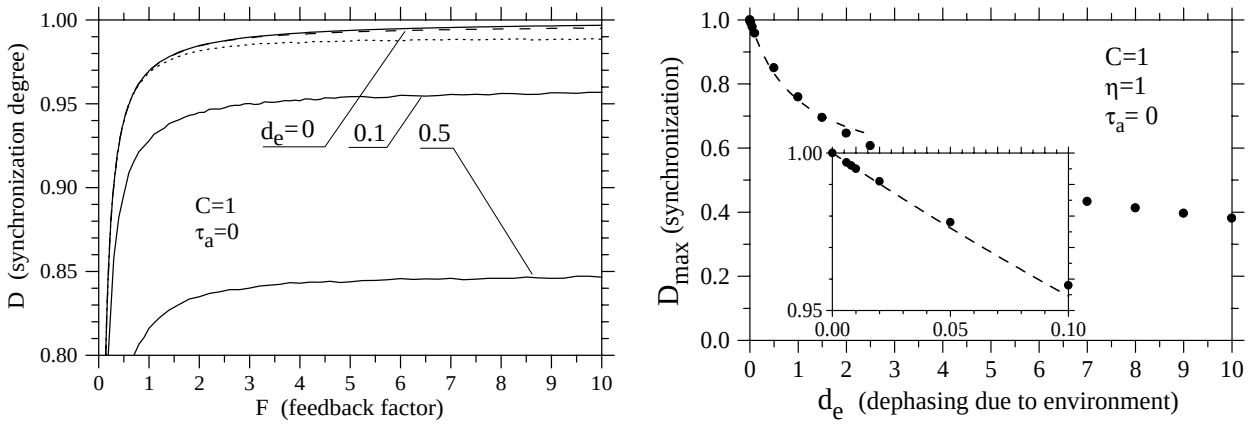

Figure 2. (a) (left panel) $D(F)$ dependence for $\mathcal{C} = 1$, $\tau_a = 0$, and several magnitudes of dephasing due to environment: $d_e = 0, 0.1$, and 0.5. Dashed and dotted lines correspond to $d_e = 0$ and limitation of H_{fb} by 0 and $H/2$, respectively. (b) (right panel) Dots: synchronization degree D_{max} at large feedback factors, as a function of dimensionless dephasing d_e due to environment. Dashed line: fitting formula $D_{max} \simeq 1 - 0.5 d_e/(1 + d_e)$. Inset shows a blow-up of the low-d_e region.

Notice that the solid lines shown in Fig. 2a as well as dots in Fig. 2b are calculated assuming the feedback control of the tunnel matrix element $H_{fb} = H(1 - F \times \Delta\phi)$ even when H_{fb} becomes negative (this is also an assumption for the analytical results). To eliminate this unphysical assumption, we have also performed numerical calculations with restriction $H_{fb} > 0$ and with restriction $H_{fb} > H/2$. This leads to rather minor modifications of the presented results (see dashed and dotted lines in Fig. 2a). However, an important difference is that with the H_{fb} restriction $D(F)$ goes down at large F, so the optimum D_{max} is achieved at some finite value of F.

3.2. Effect of Finite Detector Bandwidth

In this subsection we study the effect of the finite bandwidth $\Delta\omega$ of the line carrying the detector current $I(t)$. This parameter may be critical for possible experiments. We assume that the detector signal $I_a(t)$ available for further processing is a weighted time average of the detector current with the time constant $\tau_a \sim 1/\Delta\omega$. Here we study the model of averaging with a rectangular time window: $I_a(t) = \tau_a^{-1} \int_{t-\tau_a}^{t} I(t')dt'$. (The results for a more realistic model of an exponential time window will be presented elsewhere.) We assume that for the feedback operation $I_a(t)$ is still plugged into the Bayesian Eqs. (1)–(2) so that the "available" density matrix $\rho_a(t)$ differs from the "true" density matrix $\rho(t)$. Correspondingly, the monitored phase of oscillations is different from the actual phase. Besides the inaccuracy, we also expect some implicit time delay for the available phase ϕ_a, because the information carried by the signal, effectively comes from past moments of time. In order to compensate for this delay due to averaging, we use a modified error signal[13] $\Delta\phi = \phi_a - \Omega(t - \kappa\tau_a)$. From a simple reasoning, we would expect the optimum value $\kappa_{opt} = 1/2$ for the rectangular time window, and indeed for small coupling and not too large averaging time this value was found to provide the best operation of the feedback loop. Figure 3 shows the numerical results for the synchronization degree D calculated using $\kappa = 1/2$. As expected, finite bandwidth (finite averaging time τ_a) worsens the performance of the quantum feedback loop. The dependence $D(F)$ saturates at large F at a level which depends on τ_a and becomes significantly less than 100% when τ_a is comparable to the oscillation period $T = 2\pi/\Omega$, in which case a significant loss of information obviously occurs.

The feedback performance depends on the chosen value of the compensation parameter κ. It is easy to show that $D(\kappa)$ dependence is a sinusoidal function with a period $\Delta\kappa = T/\tau_a$, which can be parameterized as $D(\kappa) = D_{max} \cos[\Omega\tau_a(\kappa - \kappa_{opt})]$ (notice that the meaning of the notation D_{max} is different from what was used in the previous subsection). The idea of the proof is that the change of κ is equivalent to the shift of the time axis and therefore equivalent to the phase shift of $\rho_d(t)$ oscillations in the formula $D = 2\langle\rho\rho_d\rangle - 1$, while keeping $\rho(t)$ unchanged. It is important that both D_{max} and κ_{opt} (as thus the complete $D(\kappa)$ dependence) can be found within one run of the Monte-Carlo simulation by calculating two quadratures of $\rho(t)$ oscillations.

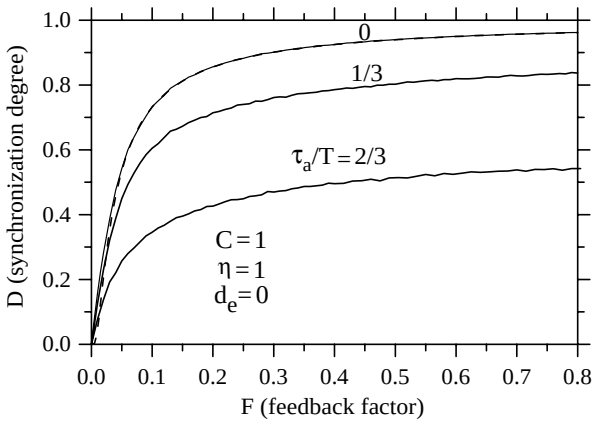

Figure 3. Dependence $D(F)$ in the case when the detector current is averaged over the rectangular time window with duration τ_a for $\tau_a/T = 0$, 1/3, and 2/3. Compensation factor $\kappa = 1/2$ is used. Analytical result $D = \exp(-\mathcal{C}/32F)$ (dashed line) almost coincides with the upper curve which assumes no averaging.

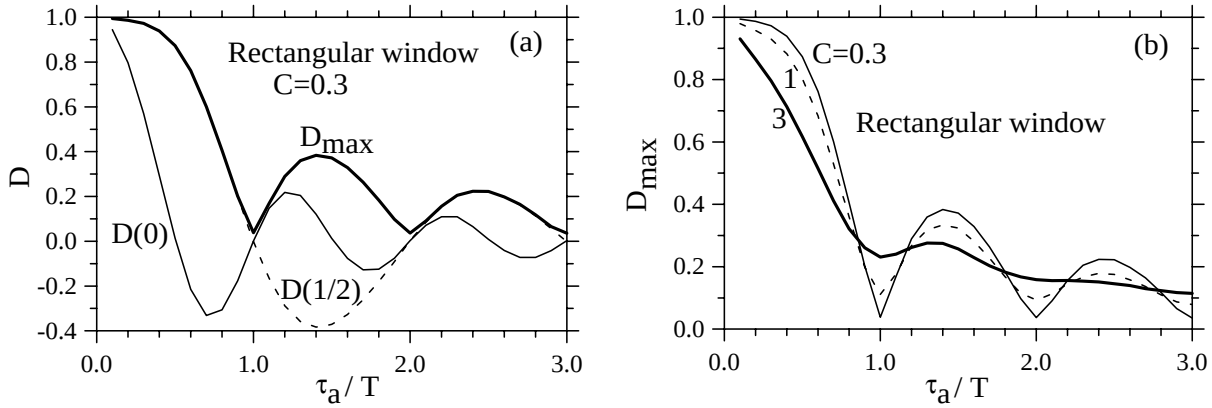

Figure 4. (a) Dependence of the qubit synchronization degree D at large F on the averaging time constant τ_a for $\kappa = 0$ (thin solid line), $\kappa = 1/2$ (dashed line) and $\kappa = \kappa_{opt}$ (thick solid line). (b) Dependence of D_{max} (for $\kappa = \kappa_{opt}$) on τ_a for several values of the qubit-detector coupling $\mathcal{C}$.

Figure 4a shows the dependence of D at large F (the saturation value with respect to F) on the averaging time constant τ_a for three choices of the parameter κ: $\kappa = 0$ (no compensation of the implicit time delay), $\kappa = 1/2$ (the most natural value used in Ref.[13]), and $\kappa = \kappa_{opt}$ (optimized value). One can see that $D(\kappa = 0)$ can be significantly smaller than $D_{max} = D(\kappa = \kappa_{opt})$ at nonzero τ_a that clearly shows the advantage of using compensation. At $\tau_a/T < 1$ the curve for $D(\kappa = 1/2)$ is quite close to the curve for D_{max} (though they do not coincide and the difference grows at larger coupling $\mathcal{C}$), which confirms that $\kappa = 1/2$ is a good choice. However, at $1 < \tau_a/T < 2$ (as well as at $2n - 1 < \tau_a/T < 2n$ with integer n) the choice $\kappa = 1/2$ leads to the π-shifted oscillations; therefore D becomes negative.

One can see that besides the overall decrease of D_{max} with increasing τ_a, the dependence $D_{max}(\tau_a)$ has an oscillating behavior and approaches values close to zero at $\tau_a = T$, $2T$, $3T$, etc. This behavior is especially pronounced at small coupling $\mathcal{C}$ and gradually smears with growing $\mathcal{C}$ as seen in Fig. 4b. A qualitative explanation is the following. At small coupling the diffusion of the phase of the Rabi oscillations is slow, so the detector signal $I(t)$ has a sinusoidal contribution with long correlation time. Averaging of such signal with the rectangular time window of duration equal to integer number of periods, practically cancels the oscillating contribution and

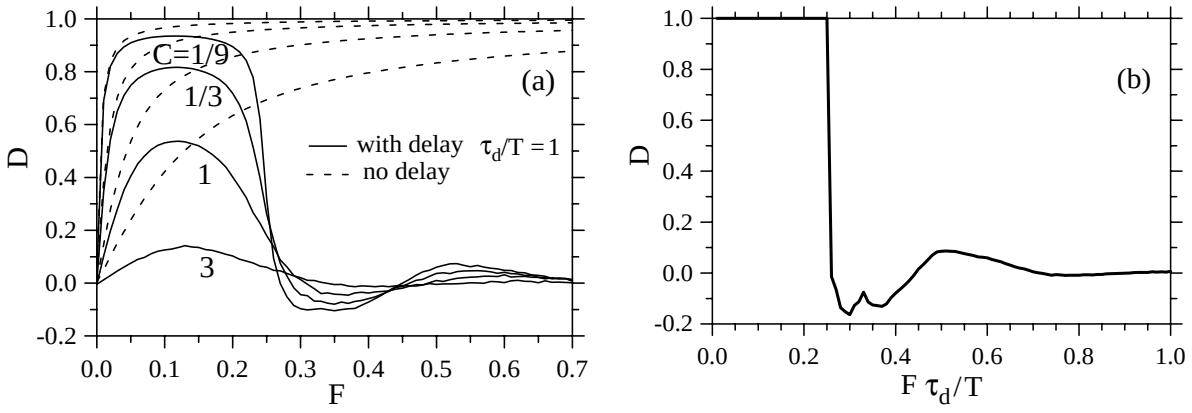

Figure 5. (a) Comparison of the results for $D(F)$ with time delay $\tau_d = T$ (solid lines) and without delay (dashed lines) for several values of the coupling $\mathcal{C}$. (b) Dependence $D(F\tau_d/T)$ calculated using the simplified model based on Eq. (13).

leads to almost complete loss of information available for the feedback control. When τ_a/T is larger than 1 but not close to an integer, the signal from the integer number of periods is also practically lost, but the remaining fractional part of the period still supplies some information used for the feedback. Notice that the oscillating behavior of $D_{max}(\tau_a)$ is a consequence of the assumption of averaging with the rectangular time window and is absent, for example, for averaging with the exponential window.

3.3. Effect of Time Delay

In a realistic feedback network the time delay within the feedback loop may have a significant effect on the feedback performance. In our case the process of solving the Bayesian equations in real time needed to monitor the quantum state of the system is probably the major source of delay; there may be also some other contributions. We model all of them with one parameter: the time delay τ_d. In this subsection we study the effect of time delay assuming infinite bandwidth ($\tau_a = 0$), ideal detector ($\eta = 1$), and absence of extra dephasing ($\gamma_e = 0$) in order to separate the effects.

The result of the delay is that at a given time moment t the available information (e.g., the monitored phase ϕ of the quantum oscillations) comes from some past moment $t-\tau_d$. Correspondingly, our linear control equation (4) becomes

$$H_{fb}(t) = [1 - F \times \Delta\phi(t - \tau_d)]H. \tag{10}$$

Solid lines in Fig. 5a show the numerically calculated dependence of the synchronization degree D on the feedback factor F for the time delay equal to the Rabi period, $\tau_d = T$, and several values of the coupling $\mathcal{C}$. For comparison, the dashed lines show the corresponding results without delay, $\tau_d = 0$. Obviously, the time delay worsens the performance of the feedback loop, leading to smaller values of D. A new feature in the $D(F)$ dependence introduced by the delay is a sharp drop of the feedback performance at $F > 1/4$ (which for our parameters also means $F\tau_d/T > 1/4$), in contrast to the monotonous increase with F in absence of delay.

To understand the physical reason of this new feature, let us start with Eq. (5) modified by introducing the delay into the feedback term:

$$\frac{d}{dt}\Delta\phi = -\sin\phi\,\frac{\Delta I}{S_0}\left(\frac{\Delta I}{2}\cos\phi + \xi(t)\right) - \frac{2FH}{\hbar}\Delta\phi(t-\tau_d). \tag{11}$$

The simplification in the weak coupling limit, $\mathcal{C} \ll 1$, leads to the equation similar to Eq. (6):

$$\frac{d}{dt}\Delta\phi(t) = \tilde{\xi}(t) - \frac{2FH}{\hbar}\Delta\phi(t-\tau_d). \tag{12}$$

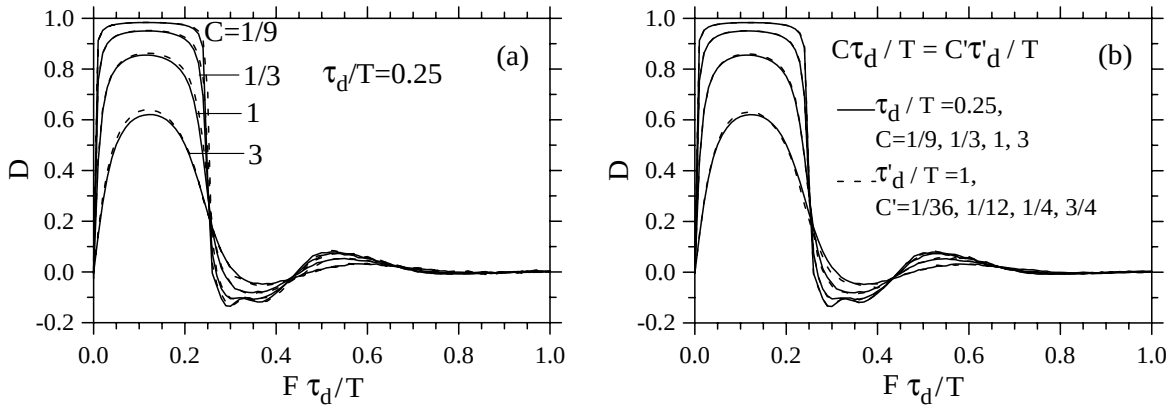

Figure 6. a) Dependence of D on F (scaled as $F\tau_d/T$) for the delay $\tau_d = T/4$ and several values of the coupling $\mathcal{C}$, calculated using the full model (solid lines) and simplified model based on Eq. (12). (b) Full model results for the $D(F\tau_d/T)$ dependence for two sets of parameters (solid and dashed lines) related by the scaling transformation discussed in the text.

As a first approximation, let us completely neglect the noise term $\tilde{\xi}$; this results in a very simple differential equation $d(\Delta\phi)/dt = -(2FH/\hbar)\Delta\phi(t-\tau_d)$. Introducing a new scaled time variable $\tilde{t} = t/\tau_d$, this equation can be further reduced to

$$\frac{d}{d\tilde{t}}\Delta\phi(\tilde{t}) = -\frac{2FH\tau_d}{\hbar}\,\Delta\phi(\tilde{t}-1) = -\frac{2\pi F\tau_d}{T}\,\Delta\phi(\tilde{t}-1). \tag{13}$$

Using the standard analysis, we try to find its solution in the form $\Delta\phi(\tilde{t}) = A\exp(\mathrm{i}\tilde{\omega}\tilde{t})$, which leads to the equation $\mathrm{i}\tilde{\omega} = -(2\pi F\tau_d/T)\exp(-\mathrm{i}\tilde{\omega})$. Its first solution for real $\tilde{\omega}$ occurs at $\tilde{\omega} = \pi/2$ and $F\tau_d/T = 1/4$, thus separating the decaying in time behavior of $\Delta\phi(\tilde{t})$ at $F\tau_d/T < 1/4$ and unstable (increasing in time) behavior at larger $F\tau_d/T$.

This simple model explains the abrupt loss of the feedback loop stability at $F\tau_d/T > 1/4$ and corresponding drop of the curves in Fig. 5a as a consequence of the "oversteering" due to too strong feedback. Figure 5b shows $D = \langle\cos\Delta\phi\rangle$ calculated numerically using Eq. (13). ($D = 1$ at $F\tau_d/T < 1/4$ because $\Delta\phi = 0$ is the stable stationary solution.) Apparent similarity of this result with the results shown in 5a confirms the validity of our simple analysis (the results should coincide in the limit $\mathcal{C} \to 0$). Notice that the nontrivial behavior at $F\tau_d/T > 1/4$ is due to modulo 2π definition of $\Delta\phi$ and assumed limitation $|\Delta\phi| < \pi$.

Since Eq. (13) has been obtained from Eq. (11) using two simplifying steps, it is interesting to analyze the inaccuracy introduced by each of them. For this purpose we have also performed the numerical calculations based on Eq. (12) which is the intermediate stage of simplification. The solid lines in Fig. 6a show the $D(F)$ dependence for the time delay $\tau_a = T/4$ calculated using the full model based on Eqs. (1)–(2) which correspond to Eq. (11), while the dashed lines show the results using Eq. (12). Even at coupling $\mathcal{C} = 3$ the difference between the solid and dashed lines is still quite small, which means that this approximation step works really well, while the second simplifying step [leading to Eq. (13) and Fig. 5b] introduces a stronger change of the results.

Since the effects of the finite bandwidth and extra dephasing are neglected in this subsection, the feedback performance D is in general some function of three dimensionless parameters: coupling $\mathcal{C}$, feedback factor F, and dimensionless delay τ_d/T. However, as we know, in absence of delay and at weak coupling, the dependence on F comes mainly through the combination $F/\mathcal{C}$, while the dependence on $\mathcal{C}$ itself is very weak [see Eq. (8)]. The effect of the time delay comes mainly through the combination $F\tau_d/T$ [see Eq. (13)]. Therefore, we would expect that in the parameterization

$$D = D(\mathcal{C},\, F/\mathcal{C},\, F\tau_d/T) \tag{14}$$

the dependence on the first argument is quite weak as long as $\mathcal{C} \ll 1$. A good feedback performance ($D \simeq 1$) in the small coupling case is expected when $F/C \gg 1$ and $F\tau_d/T < 1/4$. Notice that it automatically implies inequality $\mathcal{C}\tau_d/T \ll 1$ which can be rewritten as $\tau_d \ll \tau_{meas}$ and has an obvious physical meaning.

Parameterization Eq. (14) can be used to make the following prediction: in the weak coupling regime the scaling transformation $\mathcal{C} \to \alpha\mathcal{C}$, $F \to \alpha F$, $\tau_d/T \to \alpha^{-1}\tau_d/T$ (for arbitrary α) should not lead to a significant change of D, since it does not change the combinations $F/\mathcal{C}$ and $F\tau_d/T$. (Notice that this transformation does not change the combination $\mathcal{C}\tau_d/T = 2\tau_d/\pi\tau_{meas}$ as well.) Figure 6b confirms this prediction. The corresponding solid and dashed lines in Fig. 6b are related by the transformation with $\alpha = 4$ and show a good agreement with each other.

4. CONCLUSION

In this paper we have studied the operation of the one-qubit quantum feedback loop designed to keep the quantum coherent oscillations of a qubit for an infinitely long time, extending the results of Ref.[13] . In the ideal case (ideal detector, no extra environment, infinite bandwidth, no time delay) the theoretical fidelity of the feedback reaches 100% at $F \gg \mathcal{C}$. (Fidelity $\mathcal{F}$ is equal to $(D+1)/2$ where D is the qubit synchronization degree mostly analyzed in this paper.) The imperfections obviously decrease the fidelity.

Interaction with dephasing environment as well as the detector nonideality, limit the fidelity approximately as $\mathcal{F} \simeq 1 - 0.25 d_{tot}$ at $d_{tot} \ll 1$, where $d_{tot} = \gamma_e/[(\Delta I)^2/4S_0] + \eta^{-1} + 1$ is the ratio of the total qubit coupling to the dephasing sources (environment and the nonideal part of the detector) and the coupling to the ideal part of the detector. Even at $d_{tot} \simeq 10$ (very strong dephasing contribution) the feedback still operates with a significant efficiency ($D \simeq 0.4$, $\mathcal{F} \simeq 0.7$).

Analysis of the finite signal bandwidth has been performed using the model of signal averaging with a rectangular time window. We have found that the best compensation of the implicit time delay due to averaging is not always equal to one half of the window duration τ_a, as was previously expected. The new calculation algorithm allows us to find the best compensation factor and the corresponding fidelity in one simulation run. For the model of rectangular time window the feedback performance is found to be very inefficient ($D \simeq 0$) when τ_a is close to the integer number of oscillation periods T.

The time delay τ_d in the feedback loop also worsens the performance and may lead to the loss of the loop stability at too strong feedback. From the simplified model we have found that the threshold of instability in the case of weak coupling is $F\tau_d/T = 1/4$. The numerical simulations using the full model have confirmed this result, though finite qubit-detector coupling $\mathcal{C}$ leads to the smearing of the threshold (instability does not develop abruptly). In absence of other nonidealities except the delay, the resulting feedback fidelity is a function of three parameters: coupling $\mathcal{C}$, feedback strength F, and normalized time delay τ_d/T. An analysis of this function at $\mathcal{C} \ll 1$ leads to a conjecture of the scaling behavior (fidelity is approximately constant if parameters change as $\mathcal{C} \to \alpha\mathcal{C}$, $F \to \alpha F$, $\tau_d/T \to \alpha^{-1}\tau_d/T$), which has been confirmed numerically.

Acknowledgments

The authors thank D.V. Averin, A.C. Doherty, G.J. Milburn, and H.M.Wiseman for useful discussions. The work was supported by NSA and ARDA under ARO grant DAAD19-01-1-0491.

REFERENCES

1. C. H. Bennett, "Quantum information and computation," *Physics Today* **48**, pp. 24–30, 1995.
2. M. Nielsen and I. L. Chuang, *Quantum computation and quantum information*, Cambridge University Press, Cambridge, 2000.
3. P. W. Shor, "Scheme for reducing decoherence in quantum computer memory," *Phys. Rev. A* **52**, pp. R2493–R2496, 1995.
4. J. von Neumann, *Mathemetical foundations of quantum mechanics*, Princeton University Press, Princeton, NJ, 1955.
5. C. Ahn, A. C. Doherty, and A. J. Landahl, "Continuous quantum error correction via quantum feedback control," *Phys. Rev. A* **65**, 042301, 2002; C. Ahn, H. W. Wiseman, and G. J. Milburn, "Quantum error correction for continuously detected errors," *Phys. Rev. A* **67**, 052310, 2003.

6. K. Kraus, *States, effects, and operations: fundamental notions of quantum theory*, Lecture notes in physics, Vol. 190, Springer-Verlag, Berlin, 1993.
7. A. O. Caldeira and A. J. Leggett, "Quantum tunnelling in a dissipative system," *Ann. Phys.* (N.Y.) **149**, pp. 374–456, 1983; W. H. Zurek, "Decoherence and the transition from quantum to classical," *Physics Today* **44**, pp. 36–44, 1991.
8. C. W. Gardiner, *Quantum noise*, Springer, Heidelberg, 1991, Chap. 2.2.
9. A. N. Korotkov, "Continuous quantum measurement of a double dot," *Phys. Rev. B* **60**, pp. 5737–5742, 1999; A. N. Korotkov, "Selective quantum evolution of a qubit state due to continuous measurement," *Phys. Rev. B* **63**, 115403, 2001; A. N. Korotkov, in *Quantum noise in mesoscopic physics*, edited by Yu. V. Nazarov, Netherlands: Kluwer, 2003, pp. 205–228; cond-mat/0209629.
10. H. J. Carmichael, *An open approach to quantum optics*, Lecture Notes in Physics, Springer, Berlin, 1993.
11. H. M. Wiseman and G. J. Milburn, "Quantum theory of optical feedback via homodyne detection," *Phys. Rev. Lett.* **70**, pp. 548–551, 1993.
12. H.-S. Goan, G. J. Milburn, H. M. Wiseman, and H. B. Sun, "Continuous quantum measurement of two coupled quantum dots using a point contact: A quantum trajectory approach," *Phys. Rev. B* **63**, 125326, 2001; H.-S. Goan and G. J. Milburn, "Dynamics of a mesoscopic charge quantum bit under continuous quantum measurement," *Phys. Rev. B* **64**, 235307, 2001.
13. R. Ruskov and A. N. Korotkov, "Quantum feedback control of a solid-state qubit," *Phys. Rev. B* **66**, 041401(R), 2002.
14. R. Ruskov and A. N. Korotkov, "Entanglement of solid-state qubits by measurement," *Phys. Rev. B* **67**, 241305(R), 2003.
15. S. A. Gurvitz, "Measurements with a noninvasive detector and dephasing mechanism", *Phys. Rev. B* **56**, pp. 15215-15223, 1997.
16. E. Buks, R. Schuster, M. Heiblum, D. Mahalu, and V. Umansky, "Dephasing in electron interference by a 'which-path' detector," *Nature* **391**, pp. 871–874, 1998; D. Sprinzak, E. Buks, M. Heiblum, and H. Shtrikman, "Controlled dephasing of electrons via a phase sensitive detector", *Phys. Rev. Lett.* **84**, pp. 5820–5823, 2000; T. Hayashi, T. Fujisawa, H. D. Cheong, Y. H. Jeong, and Y. Hirayama, "Coherent manipulation of electronic states in a double quantum dot", *Phys. Rev. Lett.* **91**, 226804, 2003.
17. T. Duty, D. Gunarsson, K. Bladh, and P. Delsing, "Coherent dynamics of a Josephson charge qubit," cond-mat/0305433, 2003; A. Guillaume, J. F. Schneiderman, P. Delsing, H. M. Bozler, and P. M. Echternach, "Free Evolution of Superposition States in a Single Cooper Pair Box," cond-mat/0312544, 2003.
18. L. D. Landau and E. M. Lifsitz, *Quantum mechanics: nonrelativistic theory*, Oxford, NY, 1977.
19. A. Papoulis, *Probability, random variables, and stochastic processes*, McGraw-Hill, New York, 1991.
20. D. V. Averin, "Noise properties of the SET transistor in the co-tunneling regime," cond-mat/0010052, 2001.
21. A. A. Clerk, S. M. Girvin, and A. D. Stone, "Quantum-limited measurement and information in mesoscopic detectors", *Phys. Rev. Lett.* **67**, 165324, 2003.
22. B. Øksendal, *Stochastic differential equations*, Springer, Berlin, 1998.
23. D. V. Averin and A. N. Korotkov, "Continuous weak measurement of quantum coherent oscillations," *Phys. Rev. B* **64** 165310, 2001; A. N. Korotkov, "Output spectrum of a detector measuring quantum oscillations," *Phys. Rev. B* **63**, 085312, 2001.